Research Article | Vol. 25, No. 17 | 21 Aug 2017 | OPTICS EXPRESS 20737
Optics EXPRESS

Polarization squeezing at the audio frequency band for the Rubidium D_1 line

XIN WEN,[1,2] YASHUAI HAN,[1,2] JINYU LIU,[1,2] JUN HE,[1,2,3] AND JUNMIN WANG[1,2,3,*]

[1]*State Key Laboratory of Quantum Optics and Quantum Optics Devices, Shanxi University, Tai Yuan 030006, China*
[2]*Institute of Opto-Electronics, Shanxi University, Tai Yuan 030006, China*
[3]*Collaborative Innovation Center of Extreme Optics, Shanxi University, Tai Yuan 030006, China*
[*]*wwjjmm@sxu.edu.cn*

Abstract: A 2.8-dB polarization squeezing of the Stokes operator $\hat{S}_2$ for the rubidium D_1 line (795 nm) is achieved, with the lowest squeezing band at an audio frequency of 2.6 kHz. It is synthetized by a bright coherent beam and a squeezed vacuum, which are orthogonally polarized and share same frequency. Two methods are applied to support the optical parametric oscillator: an orthogonally-polarized locking beam that precludes residual unwanted interference and quantum noise locking method that locks the squeezing phase. Besides, the usage of low noise balanced detector, mode cleaner and the optical isolator helped to improve the audio frequency detection. The squeezing level is limited by absorption-induced losses at short wavelengths, which is 397.5 nm. The generated polarization squeezed light can be used in a quantum enhanced magnetometer to increase the measurement sensitivity.

OCIS codes: (270.6570) Squeezed states; (190.4970) Parametric oscillators and amplifiers; (190.4975) Parametric processes.

References and links

1. R. E. Slusher, L. W. Hollberg, B. Yurke, J. C. Mertz, and J. F. Valley, "Observation of squeezed states generated by four-wave mixing in an optical cavity," Phys. Rev. Lett. **55**(22), 2409–2412 (1985).
2. X. Jia, Z. Yan, Z. Duan, X. Su, H. Wang, C. Xie, and K. Peng, "Experimental realization of three-color entanglement at optical fiber communication and atomic storage wavelengths," Phys. Rev. Lett. **109**(25), 253604 (2012).
3. K. Honda, D. Akamatsu, M. Arikawa, Y. Yokoi, K. Akiba, S. Nagatsuka, T. Tanimura, A. Furusawa, and M. Kozuma, "Storage and retrieval of a squeezed vacuum," Phys. Rev. Lett. **100**(9), 093601 (2008).
4. J. Appel, E. Figueroa, D. Korystov, M. Lobino, and A. I. Lvovsky, "Quantum memory for squeezed light," Phys. Rev. Lett. **100**(9), 093602 (2008).
5. T. Eberle, S. Steinlechner, J. Bauchrowitz, V. Händchen, H. Vahlbruch, M. Mehmet, H. Müller-Ebhardt, and R. Schnabel, "Quantum enhancement of the zero-area Sagnac interferometer topology for gravitational wave detection," Phys. Rev. Lett. **104**(25), 251102 (2010).
6. B. J. Lawrie and R. C. Pooser, "Toward real-time quantum imaging with a single pixel camera," Opt. Express **21**(6), 7549–7559 (2013).
7. R. C. Pooser and B. Lawrie, "Ultrasensitive measurement of microcantilever displacement below the shot-noise limit," Optica **2**(5), 393–399 (2015).
8. F. Wolfgramm, A. Cerè, F. A. Beduini, A. Predojević, M. Koschorreck, and M. W. Mitchell, "Squeezed-light optical magnetometry," Phys. Rev. Lett. **105**(5), 053601 (2010).
9. T. Horrom, R. Singh, J. P. Dowling, and E. E. Mikhailov, "Quantum-enhanced magnetometer with low-frequency squeezing," Phys. Rev. A **86**(2), 023803 (2012).
10. N. Otterstrom, R. C. Pooser, and B. J. Lawrie, "Nonlinear optical magnetometry with accessible in situ optical squeezing," Opt. Lett. **39**(22), 6533–6536 (2014).
11. R. Schnabel, N. Mavalvala, D. E. McClelland, and P. K. Lam, "Quantum metrology for gravitational wave astronomy," Nat. Commun. **1**(8), 121 (2010).
12. J. Aasi, J. Abadie, B. P. Abbott, R. Abbott, T. D. Abbott, M. R. Abernathy, C. Adams, T. Adams, P. Addesso, R. X. Adhikari, C. Affeldt, O. D. Aguiar, P. Ajith, B. Allen, E. Amador Ceron, D. Amariutei, S. B. Anderson, W. G. Anderson, K. Arai, M. C. Araya, C. Arceneaux, S. Ast, S. M. Aston, D. Atkinson, P. Aufmuth, C. Aulbert, L. Austin, B. E. Aylott, S. Babak, P. T. Baker, S. Ballmer, Y. Bao, J. C. Barayoga, D. Barker, B. Barr, L. Barsotti, M. A. Barton, I. Bartos, R. Bassiri, J. Batch, J. Bauchrowitz, B. Behnke, A. S. Bell, C. Bell, G. Bergmann, J. M. Berliner, A. Bertolini, J. Betzwieser, N. Beveridge, P. T. Beyersdorf, T. Bhadbhade, I. A. Bilenko, G. Billingsley,

#300823 https://doi.org/10.1364/OE.25.020737
Journal © 2017 Received 23 Jun 2017; revised 12 Aug 2017; accepted 13 Aug 2017; published 16 Aug 2017

Optics EXPRESS

J. Birch, S. Biscans, E. Black, J. K. Blackburn, L. Blackburn, D. Blair, B. Bland, O. Bock, T. P. Bodiya, C. Bogan, C. Bond, R. Bork, M. Born, S. Bose, J. Bowers, P. R. Brady, V. B. Braginsky, J. E. Brau, J. Breyer, D. O. Bridges, M. Brinkmann, M. Britzger, A. F. Brooks, D. A. Brown, D. D. Brown, K. Buckland, F. Brückner, B. C. Buchler, A. Buonanno, J. Burguet-Castell, R. L. Byer, L. Cadonati, J. B. Camp, P. Campsie, K. Cannon, J. Cao, C. D. Capano, L. Carbone, S. Caride, A. D. Castiglia, S. Caudill, M. Cavaglià, C. Cepeda, T. Chalermsongsak, S. Chao, P. Charlton, X. Chen, Y. Chen, H.-S. Cho, J. H. Chow, N. Christensen, Q. Chu, S. S. Y. Chua, C. T. Y. Chung, G. Ciani, F. Clara, D. E. Clark, J. A. Clark, M. Constancio Junior, D. Cook, T. R. Corbitt, M. Cordier, N. Cornish, A. Corsi, C. A. Costa, M. W. Coughlin, S. Countryman, P. Couvares, D. M. Coward, M. Cowart, D. C. Coyne, K. Craig, J. D. E. Creighton, T. D. Creighton, A. Cumming, L. Cunningham, K. Dahl, M. Damjanic, S. L. Danilishin, K. Danzmann, B. Daudert, H. Daveloza, G. S. Davies, E. J. Daw, T. Dayanga, E. Deleeuw, T. Denker, T. Dent, V. Dergachev, R. DeRosa, R. DeSalvo, S. Dhurandhar, I. Di Palma, M. Díaz, A. Dietz, F. Donovan, K. L. Dooley, S. Doravari, S. Drasco, R. W. P. Drever, J. C. Driggers, Z. Du, J.-C. Dumas, S. Dwyer, T. Eberle, M. Edwards, A. Effler, P. Ehrens, S. S. Eikenberry, R. Engel, R. Essick, T. Etzel, K. Evans, M. Evans, T. Evans, M. Factourovich, S. Fairhurst, Q. Fang, B. F. Farr, W. Farr, M. Favata, D. Fazi, H. Fehrmann, D. Feldbaum, L. S. Finn, R. P. Fisher, S. Foley, E. Forsi, N. Fotopoulos, M. Frede, M. A. Frei, Z. Frei, A. Freise, R. Frey, T. T. Fricke, D. Friedrich, P. Fritschel, V. V. Frolov, M.-K. Fujimoto, P. J. Fulda, M. Fyffe, J. Gair, J. Garcia, N. Gehrels, G. Gelencser, L. Á. Gergely, S. Ghosh, J. A. Giaime, S. Giampanis, K. D. Giardina, S. Gil-Casanova, C. Gill, J. Gleason, E. Goetz, G. González, N. Gordon, M. L. Gorodetsky, S. Gossan, S. Goßler, C. Graef, P. B. Graff, A. Grant, S. Gras, C. Gray, R. J. S. Greenhalgh, A. M. Gretarsson, C. Griffo, H. Grote, K. Grover, S. Grunewald, C. Guido, E. K. Gustafson, R. Gustafson, D. Hammer, G. Hammond, J. Hanks, C. Hanna, J. Hanson, K. Haris, J. Harms, G. M. Harry, I. W. Harry, E. D. Harstad, M. T. Hartman, K. Haughian, K. Hayama, J. Heefner, M. C. Heintze, M. A. Hendry, I. S. Heng, A. W. Heptonstall, M. Heurs, M. Hewitson, S. Hild, D. Hoak, K. A. Hodge, K. Holt, M. Holtrop, T. Hong, S. Hooper, J. Hough, E. J. Howell, V. Huang, E. A. Huerta, B. Hughey, S. H. Huttner, M. Huynh, T. Huynh-Dinh, D. R. Ingram, R. Inta, T. Isogai, A. Ivanov, B. R. Iyer, K. Izumi, M. Jacobson, E. James, H. Jang, Y. J. Jang, E. Jesse, W. W. Johnson, D. Jones, D. I. Jones, R. Jones, L. Ju, P. Kalmus, V. Kalogera, S. Kandhasamy, G. Kang, J. B. Kanner, R. Kasturi, E. Katsavounidis, W. Katzman, H. Kaufer, K. Kawabe, S. Kawamura, F. Kawazoe, D. Keitel, D. B. Kelley, W. Kells, D. G. Keppel, A. Khalaidovski, F. Y. Khalili, E. A. Khazanov, B. K. Kim, C. Kim, K. Kim, N. Kim, Y.-M. Kim, P. J. King, D. L. Kinzel, J. S. Kissel, S. Klimenko, J. Kline, K. Kokeyama, V. Kondrashov, S. Koranda, W. Z. Korth, D. Kozak, C. Kozameh, A. Kremin, V. Kringel, B. Krishnan, C. Kucharczyk, G. Kuehn, P. Kumar, R. Kumar, B. J. Kuper, R. Kurdyumov, P. Kwee, P. K. Lam, M. Landry, B. Lantz, P. D. Lasky, C. Lawrie, A. Lazzarini, A. Le Roux, P. Leaci, C.-H. Lee, H. K. Lee, H. M. Lee, J. Lee, J. R. Leong, B. Levine, V. Lhuillier, A. C. Lin, V. Litvine, Y. Liu, Z. Liu, N. A. Lockerbie, D. Lodhia, K. Loew, J. Logue, A. L. Lombardi, M. Lormand, J. Lough, M. Lubinski, H. Lück, A. P. Lundgren, J. Macarthur, E. Macdonald, B. Machenschalk, M. MacInnis, D. M. Macleod, F. Magaña-Sandoval, M. Mageswaran, K. Mailand, G. Manca, I. Mandel, V. Mandic, S. Márka, Z. Márka, A. S. Markosyan, E. Maros, I. W. Martin, R. M. Martin, D. Martinov, J. N. Marx, K. Mason, F. Matichard, L. Matone, R. A. Matzner, N. Mavalvala, G. May, G. Mazzolo, K. McAuley, R. McCarthy, D. E. McClelland, S. C. McGuire, G. McIntyre, J. McIver, G. D. Meadors, M. Mehmet, T. Meier, A. Melatos, G. Mendell, R. A. Mercer, S. Meshkov, C. Messenger, M. S. Meyer, H. Miao, J. Miller, C. M. F. Mingarelli, S. Mitra, V. P. Mitrofanov, G. Mitselmakher, R. Mittleman, B. Moe, F. Mokler, S. R. P. Mohapatra, D. Moraru, G. Moreno, T. Mori, S. R. Morriss, K. Mossavi, C. M. Mow-Lowry, C. L. Mueller, G. Mueller, S. Mukherjee, A. Mullavey, J. Munch, D. Murphy, P. G. Murray, A. Mytidis, D. Nanda Kumar, T. Nash, R. Nayak, V. Necula, G. Newton, T. Nguyen, E. Nishida, A. Nishizawa, A. Nitz, D. Nolting, M. E. Normandin, L. K. Nuttall, J. O'Dell, B. O'Reilly, R. O'Shaughnessy, E. Ochsner, E. Oelker, G. H. Ogin, J. J. Oh, S. H. Oh, F. Ohme, P. Oppermann, C. Osthelder, C. D. Ott, D. J. Ottaway, R. S. Ottens, J. Ou, H. Overmier, B. J. Owen, C. Padilla, A. Pai, Y. Pan, C. Pankow, M. A. Papa, H. Paris, W. Parkinson, M. Pedraza, S. Penn, C. Peralta, A. Perreca, M. Phelps, M. Pickenpack, V. Pierro, I. M. Pinto, M. Pitkin, H. J. Pletsch, J. Pöld, F. Postiglione, C. Poux, V. Predoi, T. Prestegard, L. R. Price, M. Prijatelj, S. Privitera, L. G. Prokhorov, O. Puncken, V. Quetschke, E. Quintero, R. Quitzow-James, F. J. Raab, H. Radkins, P. Raffai, S. Raja, M. Rakhmanov, C. Ramet, V. Raymond, C. M. Reed, T. Reed, S. Reid, D. H. Reitze, R. Riesen, K. Riles, M. Roberts, N. A. Robertson, E. L. Robinson, S. Roddy, C. Rodriguez, L. Rodriguez, M. Rodruck, J. G. Rollins, J. H. Romie, C. Röver, S. Rowan, A. Rüdiger, K. Ryan, F. Salemi, L. Sammut, V. Sandberg, J. Sanders, S. Sankar, V. Sannibale, L. Santamaría, I. Santiago-Prieto, G. Santostasi, B. S. Sathyaprakash, P. R. Saulson, R. L. Savage, R. Schilling, R. Schnabel, R. M. S. Schofield, D. Schuette, B. Schulz, B. F. Schutz, P. Schwinberg, J. Scott, S. M. Scott, F. Seifert, D. Sellers, A. S. Sengupta, A. Sergeev, D. A. Shaddock, M. S. Shahriar, M. Shaltev, Z. Shao, B. Shapiro, P. Shawhan, D. H. Shoemaker, T. L. Sidery, X. Siemens, D. Sigg, D. Simakov, A. Singer, L. Singer, A. M. Sintes, G. R. Skelton, B. J. J. Slagmolen, J. Slutsky, J. R. Smith, M. R. Smith, R. J. E. Smith, N. D. Smith-Lefebvre, E. J. Son, B. Sorazu, T. Souradeep, M. Stefszky, E. Steinert, J. Steinlechner, S. Steinlechner, S. Steplewski, D. Stevens, A. Stochino, R. Stone, K. A. Strain, S. E. Strigin, A. S. Stroeer, A. L. Stuver, T. Z. Summerscales, S. Susmithan, P. J. Sutton, G. Szeifert, D. Talukder, D. B. Tanner, S. P. Tarabrin, R. Taylor, M. Thomas, P. Thomas, K. A. Thorne, K. S. Thorne, E. Thrane, V. Tiwari, K. V. Tokmakov, C. Tomlinson, C. V. Torres, C. I. Torrie, G. Traylor, M. Tse, D. Ugolini, C. S. Unnikrishnan, H. Vahlbruch, M. Vallisneri, M. V. van der Sluys, A. A. van Veggel, S. Vass, R. Vaulin, A. Vecchio, P. J. Veitch, J. Veitch, K. Venkateswara, S. Verma, R. Vincent-Finley, S. Vitale, T. Vo, C. Vorvick, W. D. Vousden, S. P. Vyatchanin, A. Wade, L. Wade, M. Wade, S. J. Waldman, L. Wallace, Y. Wan, M. Wang, J. Wang, X. Wang, A. Wanner, R. L. Ward, M. Was, M. Weinert, A. J. Weinstein, R. Weiss, T. Welborn, L. Wen, P. Wessels, M. West, T. Westphal, K. Wette, J. T. Whelan, S. E. Whitcomb, A. G. Wiseman, D. J. White, B. F. Whiting, K. Wiesner, C.

Optics EXPRESS

Wilkinson, P. A. Willems, L. Williams, R. Williams, T. Williams, J. L. Willis, B. Willke, M. Wimmer, L. Winkelmann, W. Winkler, C. C. Wipf, H. Wittel, G. Woan, R. Wooley, J. Worden, J. Yablon, I. Yakushin, H. Yamamoto, C. C. Yancey, H. Yang, D. Yeaton-Massey, S. Yoshida, H. Yum, M. Zanolin, F. Zhang, L. Zhang, C. Zhao, H. Zhu, X. J. Zhu, N. Zotov, M. E. Zucker, and J. Zweizig,, "Enhanced sensitivity of the LIGO gravitational wave detector by using squeezed states of light," Nat. Photonics **7**, 613–619 (2013).
13. D. Budker and M. Romalis, "Optical magnetometry," Nat. Photonics **3**, 227–234 (2007).
14. F. Hudelist, J. Kong, C. Liu, J. Jing, Z. Y. Ou, and W. Zhang, "Quantum metrology with parametric amplifier-based photon correlation interferometers," Nat. Commun. **5**, 3049 (2014).
15. K. McKenzie, M. B. Gray, P. K. Lam, and D. E. McClelland, "Technical limitations to homodyne detection at audio frequencies," Appl. Opt. **46**(17), 3389–3395 (2007).
16. M. S. Stefszky, C. M. Mow-Lowry, S. S. Y. Chua, D. A. Shaddock, B. C. Buchler, H. Vahlbruch, A. Khalaidovski, R. Schnabel, P. K. Lam, and D. E. McClelland, "Balanced homodyne detection of optical quantum states at audio-band frequencies and below," Class. Quantum Gravity **29**, 145015 (2012).
17. K. McKenzie, N. Grosse, W. P. Bowen, S. E. Whitcomb, M. B. Gray, D. E. McClelland, and P. K. Lam, "Squeezing in the audio gravitational-wave detection band," Phys. Rev. Lett. **93**(16), 161105 (2004).
18. H. Vahlbruch, S. Chelkowski, K. Danzmann, and R. Schnabel, "Quantum engineering of squeezed states for quantum communication and metrology," New J. Phys. **9**(10), 371 (2007).
19. W. P. Bowen, R. Schnabel, N. Treps, H. A. Bachor, and P. K. Lam, "Recovery of continuous wave squeezing at low frequencies," J. Opt. B **4**(6), 421–424 (2002).
20. R. Schnabel, H. Vahlbruch, A. Franzen, S. Chelkowski, N. Grosse, H. A. Bachor, W. P. Bowen, P. K. Lam, and K. Danzmann, "Squeezed light at sideband frequencies below 100 kHz from a single OPA," Opt. Commun. **240**(1-3), 185–190 (2004).
21. J. Laurat, T. Coudreau, G. Keller, N. Treps, and C. Fabre, "Compact source of Einstein-Podolsky-Rosen entanglement and squeezing at very low noise frequencies," Phys. Rev. A **70**(4), 042315 (2004).
22. W. Yang, Y. Wang, Y. Zheng, and H. Lu, "Comparative study of the frequency-doubling performance on ring and linear cavity at short wavelength region," Opt. Express **23**(15), 19624–19633 (2015).
23. L. Wu, Y. Liu, R. Deng, Z. Yan, X. Jia, and K. Peng, "Deterministic generation of bright polarization squeezed state of light resonant with the rubidium D1 absorption line," J. Opt. Soc. Am. B **33**(11), 2296–2301 (2016).
24. G. Hétet, O. Glöckl, K. A. Pilypas, C. C. Harb, B. C. Buchler, H. A. Bachor, and P. K. Lam, "Squeezed light for bandwidth-limited atom optics experiments at the rubidium D1 line," J. Phys. B **40**(1), 221–226 (2007).
25. Y. Han, X. Wen, J. He, B. Yang, Y. Wang, and J. Wang, "Improvement of vacuum squeezing resonant on the rubidium D1 line at 795 nm," Opt. Express **24**(3), 2350–2359 (2016).
26. C. Liu, J. Jing, Z. Zhou, R. C. Pooser, F. Hudelist, L. Zhou, and W. Zhang, "Realization of low frequency and controllable bandwidth squeezing based on a four-wave-mixing amplifier in rubidium vapor," Opt. Lett. **36**(15), 2979–2981 (2011).
27. N. Korolkova, G. Leuchs, R. Loudon, T. C. Ralph, and C. Silberhorn, "Polarization squeezing and continuous-variable polarization entanglement," Phys. Rev. A **65**(5), 052306 (2002).
28. J. Heersink, T. Gaber, S. Lorenz, O. Glöckl, N. Korolkova, and G. Leuchs, "Polarization squeezing of intense pulses with a fiber-optic Sagnac interferometer," Phys. Rev. A **68**(1), 013815 (2003).
29. W. P. Bowen, R. Schnabel, H. A. Bachor, and P. K. Lam, "Polarization squeezing of continuous variable Stokes parameters," Phys. Rev. Lett. **88**(9), 093601 (2002).
30. R. Schnabel, W. P. Bowen, N. Treps, T. C. Ralph, H. A. Bachor, and P. K. Lam, "Stokes-operator-squeezed continuous-variable polarization states," Phys. Rev. A **67**(1), 012316 (2003).
31. R. Tanaś and S. Kielich, "Quantum fluctuations in the Stokes parameters of light propagating in a Kerr medium," J. Mod. Opt. **37**(12), 1935–1945 (1990).
32. R. W. P. Drever, J. L. Hall, F. V. Kowalski, J. Hough, G. M. Ford, A. J. Munley, and H. Ward, "Laser phase and frequency stabilization using an optical resonator," Appl. Phys. B **31**(2), 97–105 (1983).
33. J. Xue, J. L. Qin, Y. C. Zhang, G. Li, P. F. Zhang, T. C. Zhang, and K. C. Peng, "Measurement of standard vacuum noise at low frequencies," Wuli Xuebao **65**(4), 044211 (2016).(in Chinese)
34. K. McKenzie, E. E. Mikhailov, K. Goda, P. K. Lam, N. Grosse, M. B. Gray, N. Mavalvala, and D. E. McClelland, "Quantum noise locking," J. Opt. B **7**(10), S421–S428 (2005).
35. J. Fang, R. Li, L. Duan, Y. Chen, and W. Quan, "Study of the operation temperature in the spin-exchange relaxation free magnetometer," Rev. Sci. Instrum. **86**(7), 073116 (2015).
36. E. E. Mikhailov and I. Novikova, "Low-frequency vacuum squeezing via polarization self-rotation in Rb vapor," Opt. Lett. **33**(11), 1213–1215 (2008).
37. M. Zhang, M. A. Guidry, R. N. Lanning, Z. Xiao, J. P. Dowling, I. Novikova, and E. E. Mikhailov, "Multipass configuration for improved squeezed vacuum generation in hot Rb vapor," Phys. Rev. A **96**(1), 013835 (2017).

1. Introduction

Squeezed states are prevalent in the field of quantum physics, since their first generation in 1985 [1]. With their advanced quantum features, squeezed states have been demonstrated in several applications such as, quantum information networks [2], quantum memory [3,4], and in quantum metrology and precise measurements [5–10], which are of interest to us. Early

Optics EXPRESS

experiments produced squeezing at megahertz frequencies, benefiting from the quiet noise background of the laser sources. However, in certain situations, kilohertz squeezing bands are required; for example, in gravitational wave detection (10 Hz–10 kHz) [11,12]and interaction with the atomic media [8–10]. Squeezed states at the kilohertz frequencies are required for coherent delay and storage in an electromagnetically induced transparency model, owing to the narrow transparent windows. Practical applications in bio-magnetism demand magnetic field measurements at kilohertz and below, such as in magneto-cardiography and magneto-encephalography, from a human heart or brain [13], respectively. In the developed precise measurement field, shot noise limit (SNL) of light has become the final limitation for probing. Noise reduction with sub-SNL polarization squeezed light and signal enhancement with interferometers [14] are both the possible ways to increase measurement sensitivity. In fact, squeezed-light-enhanced magnetometers have already been built in recent years. The polarization squeezed lights are obtained through squeezed vacuums that are generated from an optical parametric oscillator (OPO) [8] and an atomic ensemble via polarization self-rotation (PSR) [9] respectively. An intensity-difference squeezing is obtained by four-wave mixing (FWM) with an atomic ensemble [10]. These squeezing sources helped to increase the sensitivity in magnetic field measurements. The achieve measurement sensitivities are $32\,nT/\sqrt{Hz}$, $1\,pT/\sqrt{Hz}$ and $19.3\,pT/\sqrt{Hz}$ respectively.

In the audio frequency regime, squeezing is easily submerged in roll-up noises and the measured squeezing level is limited. Two factors limit the obtained squeezing: the technical noise induced in the detection [15,16] and squeezing degradation by the noise coupling of the control beams [17,18]. Several previous researches have revealed that parasitic interference, beam jitter, noise coupling from the local oscillator, and the imbalance in the electronic circuits are the main noise sources in squeezing measurements. In addition, the optical noises in the pump, probe, and lock beams may be induced or transmitted to the squeezed light, causing degradation. Several experimental methods have successfully pushed the squeezing band to audio frequencies. Bowen *et al*. [19] and Schnabel *et al*. [20] placed optical parametric amplifiers (OPA) in a Mach-Zehnder interferometer; such noise cancellation configurations enabled the generation of squeezed vacuums, down to 220 kHz and 80 kHz, respectively. Laurat *et al.* [21] designed a single type-II, self-phase-locked, frequency degenerate OPO and the generated two-mode squeezed state reached 50 kHz. McKenzie *et al.* [17] developed a noise dither locking technique to obtain a squeezed vacuum from 280 Hz. In their system, the OPO cavity length was not actively stabilized; hence, long-term running was impossible. The lowest squeezing achieved till date is 1 Hz [18], with two frequency-shifted control lights utilized to sense the cavity length and pump phase, respectively. This scheme eliminated parasitic interference successfully, but two separate lasers had to be used and the system was complex.

The results listed above were presented at a gravitational-wave-detection wavelength of 1064 nm; in order to interact with the atomic media, wavelengths resonant with the atomic transition lines need to be selected. For the rubidium D_1 line, as the wavelength of 795 nm is considerably shorter than 1064 nm, problems of absorption and heating arise. The reason is that the 397.5 nm pump beam is close to the lower limit of the transparent window (350-4400 nm) of the PPKTP crystal. The absorption at 795 nm is around 1%/cm, while it is 18.6%/cm [22] at 397.5 nm. This will induce additional losses, leading to the degradation of squeezing level. Heating causes instability of the cavity locking, this limits the squeezing band towards low frequencies. Several experimental attempts were made for generating polarization squeezing at 795 nm. Wolfgramm *et al.* [8] obtained a polarization squeezing of 3.6 dB at 1 MHz with the squeezing band ranging from 0.08 to 2 MHz; Wu *et al.* [23] achieved a polarization squeezing of 4 dB at an analytical frequency of 3 MHz; whereas, Hétet *et al.* [24] obtained a squeezing of 5.2 dB, covering a frequency range, 150–500 kHz. Our group achieved a-5.6 dB squeezing at 2 MHz, with a frequency band ranging from 0.2 to 10 MHz [25]. However, these results are all in the high frequency range, far away from the audio frequencies, where additional noise coupling needs to be considered. The audio-frequency squeezing at atomic wavelength is only presented

Optics EXPRESS

in atomic squeezers through PSR and FWM. Squeezed vacuum with squeezing band down to 100 Hz is achieved using the PSR with ^{87}Rb [9]; an intensity difference squeezing at 1.5 kHz is obtained via FWM, and with the modification of pump power, a broadband squeezing of 5.5-16.5 MHz can be achieved [26].

In this work, benefiting from a homemade low-noise balanced detector at audio frequencies and the improvement in the technical noises, we present a 2.8-dB polarization squeezed light, down to 2.6 kHz at the rubidium D_1 line. This result is mainly relied on the vacuum injected OPO. A polarization-perpendicular beam, which counter propagates in the cavity, is used to lock the cavity length. The quantum noise locking method is used to stabilize the squeezing phase. Besides, technical noises are carefully controlled by the low noise balanced detector, mode cleaner, the optical isolator and the ultra-stable mirror mounts. The generated polarization squeezed light can be subsequently used for precise measurements.

2. Polarization squeezing

Polarization states of lights are expressed by Stokes parameters, visualized on a Poincaré sphere. For the nonclassical states, a quantum version could be used, with Stokes operators on a quantum Poincaré sphere. The quantum Poincaré sphere is defined as:

$$\hat{S}_1^2 + \hat{S}_2^2 + \hat{S}_3^2 = \hat{S}_0^2 + 2\hat{S}_0 \tag{1}$$

Similar to its classical counterparts, each point on the Poincaré sphere represents one polarization state. The position is the mean value of the polarization vector, and the volume surrounding it represents its fluctuation [27–30].

The quantized Stokes operators are defined as:

$$\begin{aligned}
\hat{S}_0 &= \hat{a}_x^\dagger \hat{a}_x + \hat{a}_y^\dagger \hat{a}_y \\
\hat{S}_1 &= \hat{a}_x^\dagger \hat{a}_x - \hat{a}_y^\dagger \hat{a}_y \\
\hat{S}_2 &= \hat{a}_x^\dagger \hat{a}_y + \hat{a}_y^\dagger \hat{a}_x \\
\hat{S}_3 &= i(\hat{a}_y^\dagger \hat{a}_x - \hat{a}_x^\dagger \hat{a}_y)
\end{aligned} \tag{2}$$

$\hat{a}^\dagger$ and $\hat{a}$ are the photon creation and annihilation operators, subscripts x and y represent two orthogonally polarized modes.

$\hat{S}_0$ commutes with all the other three operators, while the other three operators satisfy:

$$\left[\hat{S}_1, \hat{S}_2\right] = 2i\hat{S}_3, \left[\hat{S}_2, \hat{S}_3\right] = 2i\hat{S}_1, \left[\hat{S}_3, \hat{S}_1\right] = 2i\hat{S}_2 \tag{3}$$

Thus, simultaneously exact measurement of $\hat{S}_1$, $\hat{S}_2$ and $\hat{S}_3$ are impossible. Their variances are limited by the uncertainty relations:

$$V_1 V_2 \geq \left|\left\langle \hat{S}_3 \right\rangle\right|^2, V_2 V_3 \geq \left|\left\langle \hat{S}_1 \right\rangle\right|^2, V_3 V_1 \geq \left|\left\langle \hat{S}_2 \right\rangle\right|^2 \tag{4}$$

when ' ≥ ' is replaced by ' = ', the formula represents the minimum uncertainty states.

Light is said to be polarization squeezed when the variance of one or more Stokes operators is smaller than the corresponding coherent light. Furthermore, for a tight definition, the variance of one of the Stokes operators should lies below not only the coherent limit, but also the respective minimum uncertainty state limit.

We used two orthogonally polarized fields to generate the polarization squeezing: a bright coherent light and a squeezed vacuum. The squeezed vacuum occupies the vacuum port of the coherent light. With a fixed relative phase, a sub-SNL polarization fluctuation at the orthogonal port is obtained. The diagrammatic illustrations of the quantum Poincaré sphere and the corresponding noise ball is shown in Fig. 1.

Optics EXPRESS

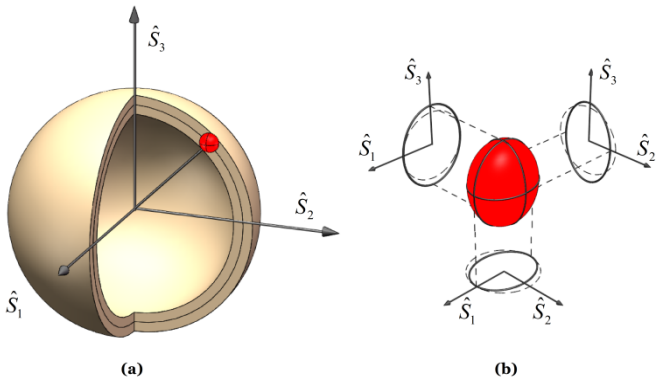

Fig. 1. (a) Illustration of the quantum Poincaré sphere. The red ball on it represents a certain polarization state. Position is given by the mean value of the polarization vector and volumes are determined by the fluctuations. (b) Diagrammatic illustration of the Stokes operators in our experiment. The red ellipsoid is the squeezed noise ball and the three ellipses are the projections at each plane. The dashed circle represents the noise of the coherent state and the solid one shows the squeezing results. The $\hat{S}_2$ operator is squeezed, the $\hat{S}_3$ operator is anti-squeezed, and that the $\hat{S}_1$ operator is the same as the coherent classical state.

Consider the situation in our experiment where *x*-polarization mode is a coherent light, *y*-polarization mode is squeezed vacuum, photon operator of the states are written as:

$$\hat{a}_x = \alpha + \delta\hat{a}_x, \hat{a}_y = \delta\hat{a}_y, \tag{5}$$

The mean values of the four Stokes operators are:

$$\left\langle \hat{S}_0 \right\rangle = \left\langle \hat{S}_1 \right\rangle = \alpha^2, \left\langle \hat{S}_2 \right\rangle = \left\langle \hat{S}_3 \right\rangle = 0 \tag{6}$$

Taking them into the uncertainty relations, we get:

$$V_1 V_2 \geq 0, V_2 V_3 \geq \alpha^2, V_3 V_1 \geq 0 \tag{7}$$

The uncertainty relations of $\hat{S}_1$, $\hat{S}_2$ and $\hat{S}_1$, $\hat{S}_3$ are bounded by zero, so both pairs commute with each other and can be obtained simultaneously and exactly. Then the $\hat{S}_2$, $\hat{S}_3$ are bounded by a nonzero limit, so they are the conjugate variances. To form a polarization squeezing, they need to satisfy:

$$V_2 < \alpha^2 < V_3 \tag{8}$$

This is the case in our scheme. Thus, a phase locked squeezed vacuum and coherent light synthetized a polarization squeezing. There have been several experiments using the same scheme [8, 31]. For similar methods, quadrature squeezed light with coherent light or two quadrature squeezed lights could both generate the polarization squeezing [29, 30]. Besides, using the nonlinear Kerr effect in glass fibers [27, 28] is also the possible way to generate polarization squeezing.

3. Improvements for squeezing towards the audio frequencies

There are many obstacles limiting the squeezing to audio frequencies, for the noise coupling leads to the roll-up of background noise levels. These technical noises have various origins, such as the laser intensity noise, photodetector electronic noise, beam jitter, parasitic interference and mechanical fluctuation. The most important source is from the laser itself. Ti:Sapphire laser has high background noise at low frequencies. The intrinsic relaxation oscillation peak of solid laser is at 1 MHz and below, this noise will be transferred to the

Optics EXPRESS

squeezed field. To avoid the noise coupling, we reduce the light injection in the cavity, for example, the probe beam. Thus, we use an OPO configuration, where only a pump field exists.

The experimental setup is displayed in Fig. 2. A low-noise continuous wave Ti:Sapphire laser works as the fundamental source. The wavelength of the laser is tuned to 794.975 nm, resonating with the rubidium D_1 line. A 30-dB optical isolator is used to avoid optical feedback. A 3.6-MHz modulation is applied to a phase-type electric optical modulator (EOM), which is used in the Pound-Drever-Hall scheme [32] for locking cavities. Two bow-tie type cavities accomplish the second harmonic generation (SHG) and the OPO successively and a third cavity, the mode cleaner (MC), is built to optimize the spatial mode of the coherent field. With the help of MC, the interference visibility is increased from 96% to 99.7% [25]. All the cavities have lengths of approximately 600 mm and a distance of approximately 120 mm between the two concave mirrors. The radii of curvature of the concave mirrors are 100 mm. A 10-mm-long periodically poled $KTiOPO_4$ (PPKTP) crystal is placed at the center of the concave mirrors and the resulting beam waist in it is approximately 40 μm. The PPKTP crystals are placed in copper-made ovens and have temperatures that are actively stabilized to approximately 53° C, for optimization. For the OPO cavity, the transmissivity of the output coupler is 11.5% at 795 nm, whereas the other three mirrors are highly reflective for the fundamental wavelength of 795 nm; the concave mirrors are highly transmissive at 397.5 nm; hence, the pump beam has a single pass through the nonlinear crystal, avoiding the extra loss owing to the absorption of ultra-violet light. The intra-cavity loss is estimated to be 0.4%, resulting in an escape efficiency of 96.6%. A homemade balanced detector is utilized, with a common-mode rejection ratio (CMRR) greater than 45 dB. It is designed for usage at audio frequencies of typically, 10 Hz–400 kHz [33]. The electric dark noise is 16 dB below the shot noise limit and the quantum efficiency of the photodiode (First Sensor, Model: PC20-7) is 95%.

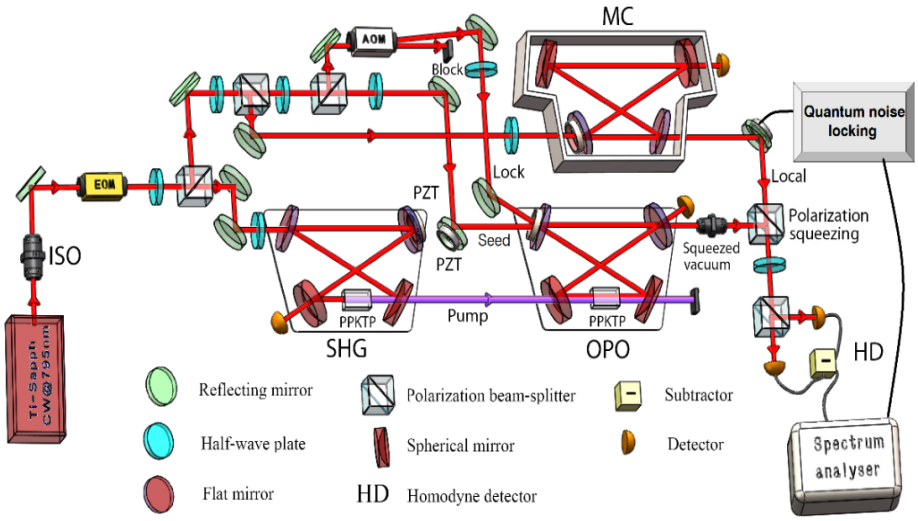

Fig. 2. Experimental setup for polarization squeezing.

To fulfill the operation of OPO, we use a 'noiseless' beam to lock the cavity length, a counter-propagating and orthogonal-polarized light. Initially, the lock beam was in a diverse direction only and worked well in the megahertz regime. However, in the audio frequency band, the residual reflection at the crystal surface will couple into the squeezed field, degrading the squeezing level. To overcome this problem, the polarization of the lock beam was changed to a p-polarization, which does not sense the OPO process. For differences between the refractive indices of the polarizations, the resonant frequency differs. In order to ensure the operation of the OPO, the cavity should be locked at the OPO resonant wavelength; hence, we use an acoustic-optical modulator to shift the frequency of the p-polarization beam to

Optics EXPRESS

approximately 140 MHz. However, a major heating source arises due to the absorption of the ultra-violet pump beam in the PPKTP crystal, which changes the cavity length; hence, the frequency of the p-polarization beam should be shifted by another 20 MHz. In addition, owing to the variation in the surrounding temperature, the frequency needs to be adjusted slightly to match with the OPO condition.

The polarization squeezing needs a phase locking of the coherent field and the squeezed vacuum. A common method relies on the interference signal of the two fields, for example, the two bright quadrature squeezing. Considering the large difference in intensity of the coherent field and the squeezed vacuum field, the interference visibility is poor. The traditional phase locking method cannot be used; thus, we turn to the quantum noise locking [34]. The configuration used is illustrated in Fig. 3. Quantum noise locking involves three steps: bandpass filtering, envelope detection, and modulation-demodulation. The settings of the resolution bandwidth (RBW) and the video bandwidth (VBW) on the spectrum analyzer (SA) select the bandwidth and the envelope detection period amplifies the real signal within a certain band. Then, the output signal is demodulated with a lock-in amplifier and the resultant error signal is fed back to a piezo-electric transducer (PZT). The noise locking method depends on the asymmetry of the phase-sensitive variances, and the stability depends on the level of squeezing and anti-squeezing.

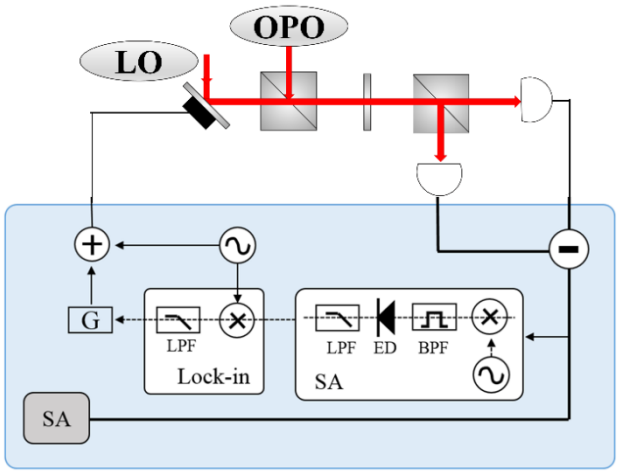

Fig. 3. Noise locking schematic; the electric part is in the blue box.

With the two techniques above, the OPO condition could be maintained, reducing the noise coupling from laser. Besides, improvements for increasing the detection efficiency and system stability are utilized. The photodetector electronic noise is reduced by the usage of the homemade balanced detector. Although commercial balanced detectors are available, for high gain and reliable stability, our homemade one is more suitable for the low frequency detection. Its quiet noise background at the measurement bands, high CMRR, and special design for the use of photodiodes with high quantum efficiency provide a solid foundation for our squeezing measurements. Beam jitter is coupled to the noise of photocurrent via spatial variation in photodetector efficiency, so a second usage of the MC is to increase the pointing stability of the coherent beam. Finally, an optical isolator is placed immediately outside the OPO cavity, precluding light being reflected back into it, from the detector surface, for instance. On one hand, light may break the locking stability of the cavity, whereas on the other, when reflected again by mirror surfaces, the following parasitic interference may contaminate the squeezing level at low frequencies. In addition, stable cavity design and usage of ultra-stable mirror mounts are also help to increase the mechanical stability.

Optics EXPRESS

4. Experimental results and discussions

Polarization squeezing of Stokes operator $\hat{S}_2$ is measured by a polarimeter, shown in Fig. 4. A half-wave plate is placed with its optical axis oriented at 22.5° to the light polarization, and a linear polarization at 45° is obtained. A polarization beam splitter (PBS) allows the measurement of the two orthogonal polarization components, and then the difference signal is send to an SA for analyzing.

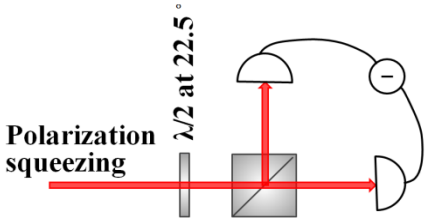

Fig. 4. Illustration of polarimeter for measurement of Stokes operator $\hat{S}_2$.

After SHG, approximately 50 mW of 397.5-nm laser is injected into the second cavity to pump the OPO. The PPKTP crystal in the OPO process is temperature controlled to 52.85 °C; and then the p-polarized locking beam is frequency shifted to match the s-polarized OPO beam. Further, the polarimeter is used to measure the polarization squeezing. We first measure the squeezing traces in a scanning mode by varying the relative phase between the squeezed vacuum and the coherent field. The results shown in Fig. 5 are at the center frequencies of 2 MHz and 50 kHz respectively. At 2 MHz, a squeezing of −5.6 dB is obtained and the anti-squeezing is + 7.0 dB; whereas at 50 kHz, the squeezing and anti-squeezing levels are −2.3 dB and + 6.6 dB, respectively. With a quantum efficiency of 95%, escape efficiency of 96.6%, propagation efficiency of 99%, and an interference visibility of 99.7%, the expected squeezing level at 2 MHz is −6.9 dB [25]. It is clear that the squeezing traces are more stable at high frequencies. However, at low frequencies, fluctuations in the optical path result in the instability of the relative phase between the squeezed vacuum and the coherent beam; thus, the noise signal dithers and cannot always stay at the lowest point.

To get a stable noise spectrum, we use the noise locking method. The generated squeezed vacuum is interfered with a coherent beam, monitored on the balanced detector. We extract the difference signal from the alternating output and send it to an SA (Agilent, Model: E4405B). The SA is set to zero span. The center frequency is 2 MHz, the RBW is 300 kHz, VBW is 30 kHz, and the sweep time is 1 s. The output of the SA is demodulated in a lock-in amplifier (SRS, Model: SR830). The modulation by the lock-in amplifier has a frequency of 35.01 kHz and an amplitude of 1.950 V. The error signal is fed back to the PZT on the coherent beam. By switching the phase in the proportional-integral-derivative controller, either a squeezed phase or an anti-squeezed phase can be achieved. The results are shown in Fig. 6.

Optics EXPRESS

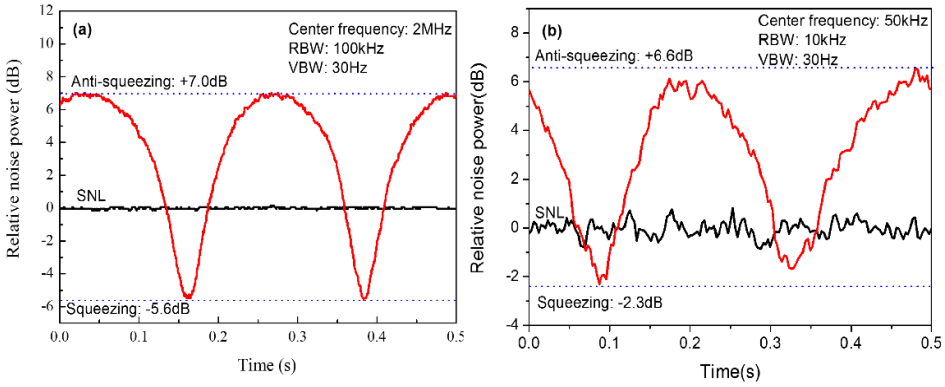

Fig. 5. Measured noise power as the phase of the coherent field is scanned. (a) Result at an analyzing frequency of 2 MHz, zero-span mode, 100 kHz RBW, and 30 Hz VBW; (b) Result at an analyzing frequency of 50 kHz, zero-span mode, 10 kHz RBW, and 30 Hz VBW. The shot noise level (SNL) trace shows the noise power with the polarized coherent beam. It gives the noise power level reference at 0 dB. In Fig. 5(a), −5.6 dB squeezing and + 7.0 dB anti-squeezing are obtained at an analyzing frequency of 2 MHz. In the Fig. 5(b), −2.3 dB squeezing and + 6.7 dB anti-squeezing are obtained at an analyzing frequency of 50 kHz. Obviously, the result at the low analyzing frequency is noisier than that at the higher analyzing frequency.

The noise traces in Fig. 6 are recorded by a second SA (Agilent, Model: 4396B). For measuring from at 1 kHz–100 kHz, the RBW is 100 Hz and the VBW is 10 Hz; in the frequency range, 2.2 kHz–3 kHz, the RBW is 10 Hz and the VBW is 1 Hz; all the noise traces are averaged 16 times. A flat noise spectrum down to 2.6 kHz is obtained and the measured squeezing level is approximately 2.8 dB. The electric noise is subtracted from the data. The peaks at approximately 19 kHz and 38 kHz are the resonant frequency of the PZT and its second harmonic, respectively; the peak at 35 kHz is the modulation frequency of the lock-in amplifier and that at 88 kHz may be owing to the extra noise in the electric circuits. Compared to the scanning mode, it is obvious that the noise locking method has a good stability.

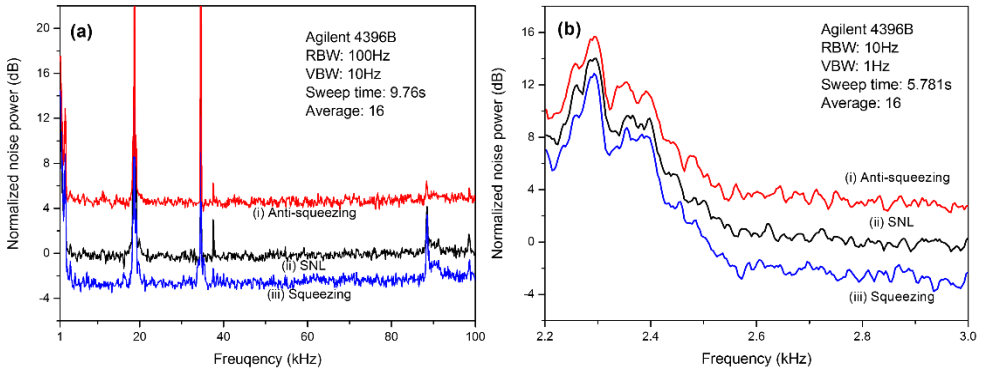

Fig. 6. Quantum noise locking results. In the frequency ranges, (a) 1 kHz–100 kHz; (b) 2.2 kHz–3 kHz. (I), (II), and (III) are the anti-squeezing, shot noise limit, and the squeezing traces, respectively. The squeezing level is approximately 2.8 dB and the flat noise spectrum, down to 2.6 kHz, is shown clearly.

The power of the polarization squeezed light is 2 mW, which is limited by the saturated power of the balanced detector. It is mainly dependent on the power of coherent beam; as the squeezed vacuum has an almost vacuum intensity, it can be ignored. The degree of polarization of the generated beam is approximately 3000:1, determined by the PBS used to synthetize the polarization squeezing.

Optics EXPRESS

At low frequency, classical noises easily coupled to the squeezing system. Although the experiments are done in a quiet environment, unexpected noises, sound, airflow or movements, enter the system randomly. These noises are uncontrollable. With imperfect CMRR, there will always be noise peaks at different frequencies. In one typical condition, where a vibration comes into only one of the detection path, there will definitely be a noise peak in the squeezing trace. Figure 7 shows one example that additional noise peak at about 68 kHz. It easily exceeds the SNL, contaminating the squeezing level. Therefore, the noise from the surroundings is one of the important factors that influence the low frequency squeezing.

As the results shown above, we obtained a polarization squeezing down to 2.6 kHz. By using the vacuum injected OPO, low noise balanced detector and some system optimization, audio-frequency noises are greatly controlled. The OPO operation is maintained by an orthogonally polarized locking beam and the quantum noise locking method. The MC used for both spatial filtering of the mode of coherent beam and relieving the influence of beam jitter. Optical isolator outside the OPO cavity prevents reflection into the cavity and is beneficial against the parasitic interference.

Compared with the lowest squeezing frequencies, the squeezed band ends at 2.6 kHz still meets some restrictions. One of the reasons is the intrinsic noise of Ti: Sapphire laser, a feedback circuit may be used to stabilize the fluctuations. Second is the roll-up of the detector electric noise, which limits extension to the lower frequencies. Thus, the balanced detector needs to be improved. Next is the imperfect mechanical stability of our bow-tie type OPO cavities. As for the severe absorption and heating problems, the standing-wave cavities with better stability are inappropriate in the short wavelengths, such as 795 nm. Hence, stabilizing the system by increasing the compactness, enclosing to avoid disturbances from the surroundings and actively isolating the fluctuations, may be beneficial.

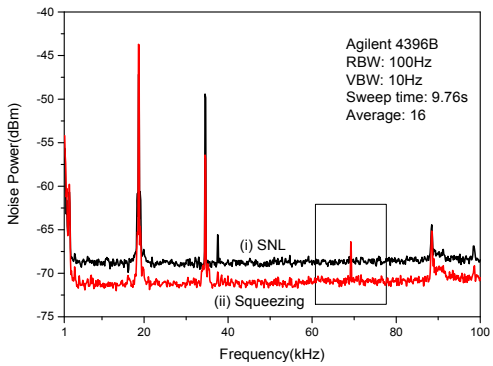

Fig. 7. Squeezing traces with additional noise peaks. Classical noises are easily couple into the low frequency range, and contaminate the squeezing. These noises randomly emerge at any frequencies and are hard to control.

5. Conclusions

We have experimentally generated an audio-frequency polarization squeezing by the combination of a bright coherent beam and a squeezed vacuum. A flat noise spectrum as low as 2.6 kHz was obtained with a squeezing level of 2.8 dB. A vacuum injected OPO is utilized, which reduced the laser intensity noise that coupled to the squeezed field. Two methods are used to maintain the OPO operation: an orthogonal-polarized, frequency-shifted locking beam and the quantum noise locking method. Then, the low noise balanced detector, mode cleaner and the optical isolator are also helped to improve the audio frequency detection. It is difficult to further extend the squeezing band to lower frequencies, where more severe requirements for vibration isolation or noise reduction are expected. Enhancing the system stability and careful control of the cavity loss may enable an increase in the squeezing level. After locking the

Optics EXPRESS

relative phase between the squeezed vacuum and the coherent beam, the coherent beam obtains a considerably quieter noise background at its orthogonal port.

In future, we intend to use this polarization squeezed light as the probe beam in a magnetic field sensor, in which they need to be far off-resonant in order not to disturb the prepared atomic states. In a previous experiment of a spin-exchange relaxation free magnetometer, the probe beam is detuned even 0.3 nm to an atomic transition line [35]. For an OPO system, the broad bandwidth of parametric gain in nonlinear crystal can be achieved just by fine adjustment of the crystal's temperature, so the squeezing level is not affected in a wide wavelength range. Thus a tunable polarization squeezing is achieved, which could satisfy various atomic systems. Compared with an atomic squeezer, although the latter seems simpler than the OPO scheme, the squeezing wavelength is always limited. An optimized squeezing level is achieved at a particular frequency [26, 36], so the adjustable frequency detuning is difficult to fulfill in such an atomic squeezer. Thus, the OPO system is more advantageous in a real magnetometer. In addition, the squeezing level from a PSR is far below the OPO (both systems generate the squeezed vacuum). In a PSR, the maximum squeezing achieved is 2.6 dB in a multipass configuration [37], while it is 5.6 dB in our OPO system. When propagating through the atomic media in the magnetometer, the squeezing level of this probe beam will surely degrade due to the absorption and dispersion losses, so a high squeezing level should be expected. The squeezing level of OPO is another advantage over the PSR system. With the help of polarization squeezed light, the weak magnetic signal will emerge from the squeezed noise spectrum, achieving an enhanced signal-to-noise ratio and increasing the measurement sensitivity.

Funding

National Natural Science Foundation of China (NSFC) (61227902 and 61475091) and National Key Research and Development Program of China (2017YFA0304502).